European Journal of Medicinal Chemistry 46 (2011) 2797–2806

Contents lists available at ScienceDirect

European Journal of Medicinal Chemistry

journal homepage: http://www.elsevier.com/locate/ejmech

Original article

Identification of 5-arylidene-4-thiazolidinone derivatives endowed with dual activity as aldose reductase inhibitors and antioxidant agents for the treatment of diabetic complications

Rosaria Ottanà [a,*], Rosanna Maccari [a], Marco Giglio [a], Antonella Del Corso [b], Mario Cappiello [b], Umberto Mura [b], Sandro Cosconati [c], Luciana Marinelli [c], Ettore Novellino [c], Stefania Sartini [d], Concettina La Motta [d], Federico Da Settimo [d]

[a] Dipartimento Farmaco-chimico, Università di Messina, Polo Universitario Annunziata, 98168 Messina, Italy
[b] Dipartimento di Biologia, Unità di Biochimica, Università di Pisa, Via S. Zeno 51, 56127 Pisa, Italy
[c] Dipartimento di Chimica Farmaceutica e Tossicologica, Università di Napoli "Federico II", Via D. Montesano 49, 80131 Napoli, Italy
[d] Dipartimento di Scienze Farmaceutiche, Università di Pisa, Via Bonanno 6, 56126 Pisa, Italy

ARTICLE INFO

Article history:
Received 26 December 2010
Received in revised form
20 March 2011
Accepted 23 March 2011
Available online 8 April 2011

Keywords:
Diabetes mellitus
Aldose reductase
Antioxidant agent
5-arylidene-4-thiazolidinones
Molecular docking

ABSTRACT

In continuing the search for more effective 5-arylidene-4-thiazolidinones as aldose reductase inhibitors, a new set of suitably substituted compounds (**4**, **5** and **8**) was explored. Acetic acids **5**, particularly **5a** and **5h**, proved to be interesting inhibitors of the enzyme as well as excellent antioxidant agents that are potentially able to counteract the oxidative stress associated with both diabetic complications as well as other pathologies. Molecular docking experiments supported SAR studies.

1. Introduction

Diabetes mellitus (DM) is a common chronic disease in constant growth that is taking on epidemic proportions especially in developing countries. More than 220 million people worldwide suffer from DM and this figure is expected to increase to 400 million cases by 2030 [1]. Diabetic complications, such as neuropathy, retinopathy, nephropathy or cataract, are serious and disabling pathologies associated with DM [2]. Hyperglycemia is a typical condition of DM and plays a crucial role in the development and advancement of these complications which arise from acute and reversible changes in cellular metabolism as well as from irreversible long-term damage in biological macromolecules.

Prospective studies have highlighted that good control of blood glucose levels delays the onset or slows the progression of diabetic complications [3]. Despite the wide availability of effective oral antidiabetic drugs, it is difficult to keep glycemia under tight control and thus the onset of long-term damage is unavoidable. Considerable efforts have been made to identify effective agents that are able to counteract the biological mechanisms responsible for the development of diabetic complications but so far very few drugs have been marketed [4]. Among the numerous mechanisms triggered by the chronic exposure to high levels of glucose the ones that are very clearly related to hyperglycemia are non-enzymatic glycation of proteins, glucose auto-oxidation, the activation of protein kinase C (PKC) isoforms and the polyol pathway [5]. Moreover these biochemical pathways sustain in various tissue types the increase in hyperglycemic-induced oxidative stress which is observed in both clinical and experimental DM and leads to the deleterious effects on cellular functions and signaling underlying the appearance of both macro- and microangiopathy [5–8]. In

Abbreviations: AD4, AutoDock4; AGE, advanced glycation end-product; ALR2, aldose reductase; ARI, aldose reductase inhibitor; DM, diabetes mellitus; GSH, glutathione; HNE, 4-hydroxy-2-nonenal; MDA, malondialdehyde; NF-κB, nuclear factor-κB; PKC, protein kinase C; ROS, reactive oxygen species; TBARS, thiobarbituric acid reactive substances.

* Corresponding author. Tel.: +39 90 6766408; fax: +39 90 6766402. .
E-mail address: ottana@pharma.unime.it (R. Ottanà).

0223-5234/$ – see front matter © 2011 Elsevier Masson SAS. All rights reserved.
doi:10.1016/j.ejmech.2011.03.068

hyperglycemic conditions, the auto-oxidation reactions of glucose and other α-hydroxyaldehydes produce reactive oxygen species (ROS) which can damage biomolecules, cellular membranes and tissues by promoting intermolecular cross-linking and fragmentation reactions as well as lipid oxidation [5,6]. Moreover the highly reactive dicarbonyl compounds produced in the course of glucose auto-oxidation reactions lead to the glycation of macromolecules which culminates in the synthesis of advanced glycation end-products (AGEs) [7,8]. The binding of AGEs to their cell surface receptors gives rise to signal transduction events culminating in the activation of nuclear factor-kB (NF-kB) which in turn sustains the development of DM-associated vascular pathologies by increasing TNFα production [5,7,8]. Within the complex pathway of AGE formation, 3-deoxyglucosone is an important intermediate among the highly reactive dicarbonyl compounds. It is mainly produced from fructose, which originates above all via the polyol pathway, thus it represents a key link between AGE formation and polyol pathway activation [9].

In hyperglycemic conditions the significant increase of glucose flux through the polyol pathway increases both cellular oxidative and osmotic stress, thereby significantly contributing to tissue injury linked to DM [4,5,7] particularly in tissues involved in the diseases associated with DM in which the glucose up-take is insulin-independent. Aldose reductase (E.C.1.1.1.21) (ALR2), a ubiquitous enzyme which has been identified in brain, kidney, liver, lens and skeletal muscle tissue, is an aldo-keto reductase that catalyzes the NADPH-dependent reduction of glucose into sorbitol in the first step of the polyol pathway. In turn, sorbitol is converted into fructose by sorbitol dehydrogenase through an NAD^+-dependent reaction. Although not determinant, the osmotic stress generated by sorbitol accumulation has been proposed as contributing to the development of tissue damage above all in the lens [10,11]. Moreover, the increase in the NADH/NAD^+ ratio promotes the activation of PKC isoforms which are found to be crucial mediators of biochemical and functional alterations triggered by hyperglycemia. Furthermore, the depletion of the NADPH cofactor reduces the activity of NADPH-requiring enzymes such as glutathione (GSH) reductase. The substantial decrease in the level of GSH, which is involved in several critical reductive metabolic steps, is also associated with a concomitant rise in the level of toxic lipid peroxidation products such as malondialdehyde (MDA) and trans-4-hydroxy-2-nonenal (HNE) [11]. Thus, the oxidative stress triggered by the glucose-oxidation process and upheld by increased ALR2 activity is rightly considered to be a major and unifying mechanism responsible for the onset of diabetic complications [5].

In addition, recent evidence has shown ALR2 to be involved in downstream pathways induced by various stimuli, such as cytokines, growth factors and lipopolysaccharides. In fact, by catalyzing the reduction of the conjugate GS-HNE to the corresponding GS-dihydroxynonene, the enzyme is involved in the transduction of inflammatory signaling via PKC activation [11,12]. The subsequent activation of NF-kB culminates in the expression of inflammatory mediators such as TNFα, IL1β and COX-2. Compelling evidence demonstrates that ALR2 inhibition extinguishes NF-kB signaling by blocking PKC activation [12]. As it is implicated in numerous overlapping and intersecting biochemical pathways, ALR2 inhibition therefore represents an intriguing strategy by which to prevent and/or arrest the progression of long-term diabetic complications [5,10]. In view of the complex metabolic changes induced by hyperglycemia in which ALR2 is critically involved and the prominent role performed by oxidative stress, derivatives endowed with dual activity as ALR2 inhibitors and antioxidant agents could thus represent a promising way forward in the search for useful drugs to treat long-term complications associated with DM. A variety of structurally different compounds have already been identified as potent in vitro ALR2 inhibitors (ARIs) [13]. They can be classified into three general groups based on their structures: acetic acid derivatives (e.g. tolrestat and epalrestat), cyclic imides (especially spirohydantoins, e.g. sorbinil) and phenolic derivatives (e.g. quercetin) (Fig. 1). Despite being structurally different, all ARIs possess two peculiar pharmacophoric elements: a) an acid moiety which is able to interact with the rigid anion binding site of the catalytic site (Y48, H110, W111 and the flanking cofactor $NADP^+$) and b) a lipophilic scaffold which can bind to the flexible specificity pocket of the catalytic site lined with L300, W111, T113 [14]. In spite of the numerous efforts made over recent decades, to date epalrestat is the only ARI currently available on the market and in Japan alone. Clinical trials of several ARIs highlighted an inadequate therapeutic index attributable to serious adverse effects as well as to pharmacokinetic problems linked to poor therapeutic effectiveness [4]. In this context, 2,4-thiazolidinediones have attracted considerable attention being ARIs designed as sorbinil analogues that lack the hydantoin moiety which is thought to be responsible for side effects. Among the 2,4-thiazolidinediones, several derivatives exhibit interesting ability as ARIs [4,13]. Moreover, the introduction of 2,4-thiazolidinediones into clinical practice as antidiabetic drugs that are able to improve glycemic control and enhance insulin sensitivity in type 2 diabetic subjects, has increased the interest in this class of compounds as potential dual purpose drugs to treat both DM and its associated complications.

In recent years, we have designed a series of 5-arylidene-2,4-thiazolidinones active as ARIs [15] (Fig. 1). Among these, compounds **1**–**2** proved to be excellent in vitro inhibitors, reaching IC_{50} values in the micromolar and submicromolar range. The presence of an acetic chain N-3 gave inhibitors **2** which were found to be endowed with the highest activity. The corresponding N-unsubstituted analogues **1** proved to be interesting ALR2 inhibitors despite not achieving the effectiveness of compounds **2** [15a].

The substituents on the 5-arylidene moiety are found to significantly influence the inhibitory ability. In particular, the presence of a wide lipophilic moiety, such as phenoxybenzylidene, benzyloxybenzylidene or naphthylmethylidene, favors interaction with the ALR2 lipophilic pocket.

Molecular docking experiments of 2,4-thiazolidinediones into the ALR2 active site highlighted that the acetic acid group can bind the anion binding site by electrostatic and hydrogen bonds with Y48, H110 and W111 together with the nicotinamide moiety of the cofactor, while the lipophilic 5-arylidene group binds tightly to the hydrophobic binding pocket lined with W111 and L300 [15a–c].

The results acquired for this class of inhibitors prompted us to synthesize and test new and more lipophilic derivatives in which targeted structural modifications were introduced in the 5-arylidene moiety while keeping unchanged the acetic chain on N-3.

We now report the synthesis of compounds **4** and **5** (Scheme 1). These were designed in order to evaluate the effects brought about by the introduction of a new linker (e.g. the vinyl moiety) between the two aromatic rings or between the methylidene group and the aromatic ring of the arylidene moiety. The insertion of this spacer also allowed a more extensive electronic delocalization which could strengthen the affinity of inhibitors with ALR2 through different interactions. In addition, the introduction of the vinyl moiety could serve as a probe to assess the capability of the flexible lipophilic pocket of ALR2 to accommodate an enlarged arylidene moiety. The substituents inserted on the para position of the distal aromatic ring were selected on the basis of their different electronic characteristics. Compounds **4g** [16], **4e** [17] and **5e** [18] are already been described but, to the best of our knowledge, only compound **5e** has so far been reported as an ARI in a patent. The latter was included in this study for completeness of the SAR study. In the

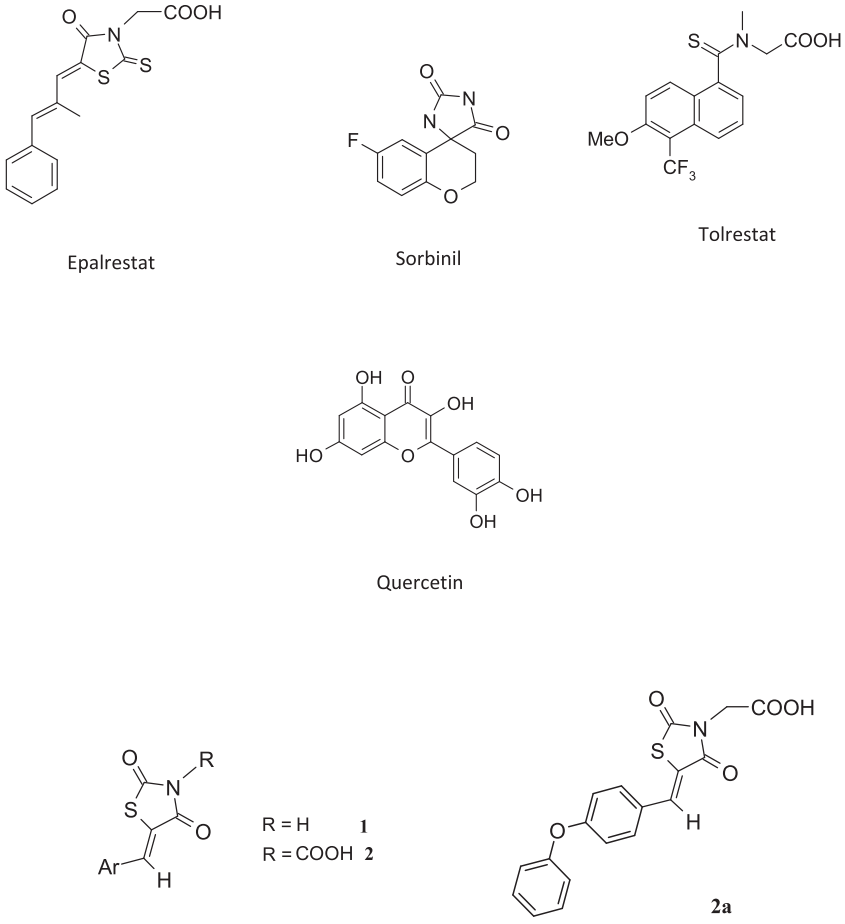

Fig. 1. Known ALR2 inhibitors.

context of the synthesis of more lipophilic 5-arylidene-2,4-thiazolidinediones derivatives, 2-phenylimino analogues **8** (Scheme 2) were designed in order to evaluate the effect of an additional aromatic ring inserted into position 2 of the thiazolidinone system on ALR2 inhibitory ability. In acids **8i-k**, the 5-arylidene moieties bore two aromatic rings like the previously tested 2,4-thiazolidinediones [15a,c,d]. The presence of functional groups that were susceptible to oxidation or to act as radical scavengers also prompted us to evaluate the antioxidant proprieties of the 5-arylidene-2,4-thiazolidinediones endowed with the best ALR2 inhibitory ability. Docking experiments into the binding site of ALR2 supported the rationalization of the in vitro experimental results.

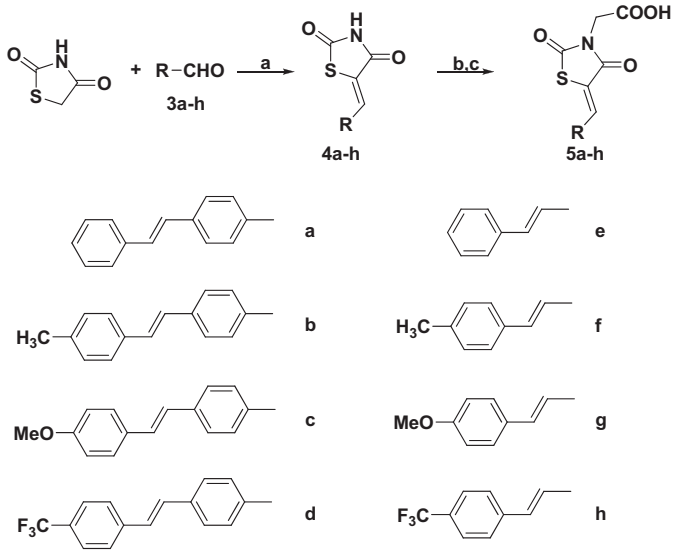

Scheme 1. Synthesis of inhibitors **4** and **5**. Reagents and conditions: (a) $C_5H_{11}N$, EtOH, Δ; (b) K_2CO_3, acetone, $BrCH_2COOCH_3$, Δ; (c) AcOH, HCl, Δ.

2. Chemistry

The synthesis of compounds **4** and **5** was carried out following the procedure depicted in Scheme 1. 2,4-Thiazolidinediones **4a**–**h** were obtained via Knoevenagel condensation of the commercially available 2,4-thiazolidinedione and suitably substituted aldehydes **3a**–**h**, in ethanol at reflux in the presence of piperidine. The reaction of N-alkylation of compounds **4** with methyl bromoacetate under basic conditions provided the intermediate methyl esters that gave the corresponding acetic acids **5** by hydrolysis in concentrated hydrochloric acid and glacial acetic acid.

The synthesis of (5-arylidene-4-oxo-2-phenyliminothiazolidin-3-yl)acetic acids (**8**) was carried out by means of a multistep procedure which was developed for previously reported analogues [19] (Scheme 2). The [(phenylcarbamothioyl)amino]acetic acid (**6**) was obtained by the reaction of phenylisothiocyanate and aminoacetic acid in a hydroalcoholic solution at reflux under basic conditions. The condensation of **6** with chloroacetyl chloride in the presence of triethylamine in refluxing ethanol afforded the intermediate (4-oxo-2-phenyliminothiazolidin-3-yl)acetic acid (**7**). As

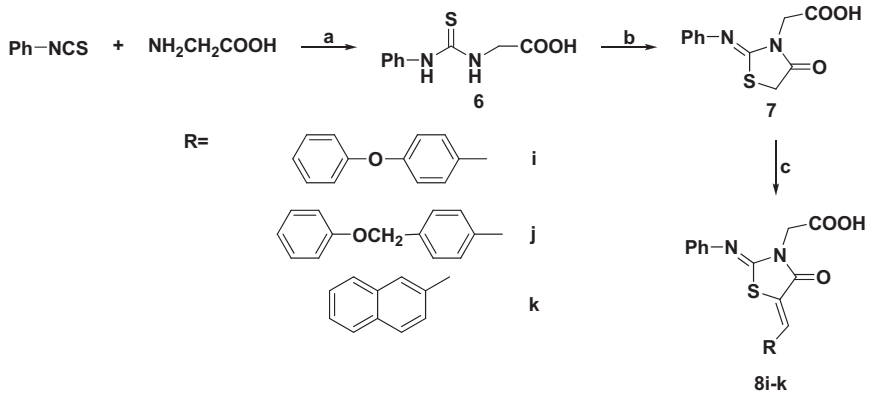

Scheme 2. Synthesis of compounds **8**. Reagents and conditions: (a) EtOH/H_2O, Δ; (b) $ClCH_2COCl$, Et_3N, EtOH, Δ; (c) ArCHO, $C_5H_{11}N$, EtOH, Δ.

previously reported [19], 2-phenylimino isomer is the only one allowed from N-aryl-N′-alkyl-substituted thioureas under the experimental conditions reported. Finally, the Knoevenagel condensation of compound **7** with appropriate aromatic aldehydes, using piperidine as the base in refluxing ethanol, provided (5-arylidene-4-oxo-2-phenyliminothiazolidin-3-yl)acetic acids (**8i**–**k**).

3. Results and discussion

The in vitro ALR2 inhibitory activity of compounds **4**, **5** and **8** was assessed using the highly purified enzyme from bovine lens (Table 1). D,L-glyceraldehyde was employed as substrate while sorbinil and epalrestat were used as reference drugs. For comparison purposes, the ALR2 inhibitory activity of compound **2a** (Fig. 1) was also evaluated, as this had been shown to be a potent inhibitor of partially purified bovine lens ALR2 (IC_{50} = 0.82 μM) [15a], and had displayed an even lower IC_{50} value (0.070 μM) against highly purified lens ALR2. The in vitro inhibition data (Table 1) show that the tested compounds proved generally to inhibit ALR2. Of these, (5-arylidene-2,4-dioxothiazolidin-3-yl)acetic acids **5** were the best inhibitors, with IC_{50} values ranging between 0.25 μM (**5c**) and 1.32 μM (**5e**), thus confirming the crucial role played by the acetic acid group in the interaction with the enzyme. All compounds **5** resulted as being more active than sorbinil and, among them, **5a**, **5c** and **5h**, showed activity levels similar to that of epalrestat (Table 1).

Of compounds **5**, the styrylbenzylidene derivatives **5a-c**, characterized by IC_{50} values ranging between 0.25 μM and 0.35 μM, proved to be more effective ALR2 inhibitors than corresponding styrylmethylidene series **5e**–**g** (IC_{50} 0.85–1.32 μM). These results were in close agreement with the previously acquired SARs indicating that a wider 5-arylidene moiety may be important for activity in general as it provided the best inhibitors of this class of compounds [15].

The selected substituents inserted on the aromatic ring of the portion in position **5** were found to produce opposite effects on the ALR2 inhibitory activity of the two series of compounds (**5a**–**d** and **5e**–**h**). In fact, within the inhibitory activity of styrylbenzylidene derivatives **5a**–**d**, the effects triggered by the introduction of a methyl (**5b**, IC_{50} 0.35 μM) or methoxy (**5c**, IC_{50} 0.25 μM) group in the para position of the distal phenyl ring proved to be indifferent or negligible for the affinity with ALR2 in comparison with the corresponding unsubstituted derivative **5a** (IC_{50} 0.27 μM). In contrast, the presence of a trifluoromethyl group on the same position (**5d**) was found to induce a clear detrimental effect increasing the IC_{50} value to 1.25 μM.

The removal of the vicinal phenyl ring (**5e**–**h**) resulted in the reversal of the behavior observed for compounds **5a**–**d**. In fact, the 4-trifluoromethylstyrylmethylidene substituted derivative (**5h,** IC_{50} 0.30 μM) proved to be 4-fold more active than the corresponding styrylbenzylidene analogue (**5d**) whereas the unsubstituted analogue **5e** was the worst inhibitor of not only compounds **5e**–**h**, but also of all compounds **5**.

The removal of the acetic chain on N-3 afforded compounds **4** which were found to be weaker ALR2 inhibitors than compounds **5**. Within the series of derivatives **4**, the insertion of an additional phenyl ring in the 5-arylidene moiety led to the opposite effect compared with that seen for analogues **5**. In fact, styrylmethylidene analogues **4e**–**h** proved to be better ALR2 inhibitors than the corresponding styrylbenzylidene derivatives **4a**–**d**.

In addition, the comparison of ALR2 inhibitory ability of the two series of compounds **4e**–**h** and **5e**–**h** indicated that the same substituents inserted on phenyl ring determined a similar pattern of activity.

2-Phenylimino substituted compounds **8i**–**k** displayed activity in the low micromolar range (2.7–4.4 μM) and, of these the most active (IC_{50} 2.7 μM) was the [5-(naphtalen-2-ylmethylidene)-4-oxo-2-phenyliminothiazolidin-3-yl]acetic acid (**8k**). They showed higher IC_{50} values than the analogous 2,4-thiazolidinediones previously reported [15a]. In particular, the 4-phenoxybenzylidene analogue **8i** (IC_{50} 4.4 μM) was found to be 63-fold less active than the corresponding 2,4-thiazolidinedione **2a** (Table 1). Compound **2a** and the analogous 5-(4-benzyloxybenzylidene)-2,4-(dioxothiazolidine-3-yl)acetic acid showed to be more active (IC_{50} 0. 82 μM and 0. 28 μM, respectively) [15a] even when tested against partially purified ALR2. On the basis of these results, it is conceivable that the additional 2-phenylimino moiety prevented the effective fit of compounds **8** with the aminoacids surrounding the active site, thereby decreasing the affinity with ALR2.

Table 1
In vitro bovine lens ALR2 inhibitory activity of compounds **4**, **5** and **8**.

Compd	IC_{50} (μM)	Compd	IC_{50}(μM)
4a	n.i.	**5a**	0.27 (0.15–0.49)
4b	39%[a]	**5b**	0.35 (0.13–0.96)
4c	n.i.	**5c**	0.25 (0.11–0.60)
4d	29%[a]	**5d**	1.25 (0.74–2.08)
4e	31%[a]	**5e**	1.32 (0.54–3.24)
4f	46%[a]	**5f**	1.05 (0.51–2.13)
4g	51%[a]	**5g**	0.85 (0.49–1.48)
4h	65%[a]	**5h**	0.30 (0.13–0.70)
Sorbinil	2.0 (1.70–3.50)	**8i**	4.40 (3.30–6.00)
Epalrestat	0.17 (0.09–0.34)	**8j**	4.90 (3.03–8.00)
2a	0.070 (0.033–0.16)	**8k**	2.70 (1.40–5.42)

[a] % inhibition at 25 μM; n.i. = no inhibition at 25 μM.

The most effective ALR2 inhibitors, **5a**–**h**, were also investigated as regards their antioxidant properties, by examining their effects on hydroxyl radical-dependent lipoperoxidation induced in rat brain homogenate by the oxidant system Fe(III)/ascorbic acid. All the tested compounds exhibited excellent antioxidant properties. Actually, when tested at a final concentration of 100 μM, they proved to inhibit the production of thiobarbituric acid reactive substances (TBARS), assumed as an index of lipid peroxidation and expressed as nmol of MDA obtained *per* mg of tissue. Moreover, they emerged as being significantly more effective than the chain-breaking antioxidant α-tocopherol [20], used as the reference standard (Fig. 2). In the styrylbenzylidene series (**5a**–**d**), the insertion of electron-releasing substituents on the distal phenyl ring led to a slight reduction of activity compared with the unsubstituted analogue **5a**. In fact, passing from **5a** to **5c** we observed a progressive increase in the production of TBARS. Conversely, the insertion of the electron-withdrawing trifluoromethyl group interrupted this negative pattern, with derivative **5d** proving to be as effective as the unsubstituted **5a**.

Regarding the 5-(3-phenylpropenylidene) series (**5e**–**h**), the insertion of both electron-releasing and electron-withdrawing substituents in the para position of the phenyl group produced a general increase in the antioxidant properties with respect to the unsubstituted analogue **5e**, thus the substituted compounds **5f**–**h** were found to be nearly equipotent. Also in this series, the insertion of the electron-withdrawing trifluoromethyl group turned out to be an effective choice, as compound **5h** was shown to be an interesting antioxidant agents. Interestingly, for compounds **5a** and **5h**, the effectiveness as ALR2 inhibitors is associated with high activity as ROS scavenging molecules.

3.1. Molecular modeling

In order to gain greater insight into the interaction mode of compounds **5**, docking calculations were performed on compounds **5c** and **5h**, which proved to be the most potent ALR2 inhibitors in the two series of compounds **5a**–**d** and **5e**–**h**. It is well known that ALR2 can adopt at least three main different binding site conformations depending on the ligand [14b]. Thus, a "sorbinil conformation" (PDB code 2PDK), an "IDD594 conformation" (PDB code 2PDK) and "tolrestat conformation" (PDB code 2FZD) exist. In particular, the ARL2 binding site can be divided into two different regions having diverse plasticity properties. The first, which could be considered the most rigid one, is named "anion binding pocket" and is made up of the catalytic site and the flanking cofactor. Conversely, the second, known as specificity pocket, flanked by W111 indole, displays a high degree of flexibility, especially regarding V297-L300, W219, C303, and Y309 residue side chains (Fig. 3). To include such a plasticity in our calculations the "ensemble docking" approach was adopted. Indeed, an advanced version of this approach employing AutoDock4 (AD4) software as the search engine [21], has been recently employed in a virtual screening campaign achieving a high success rate [22]. Accordingly, calculations with AD4 were also used in the present study to dock **5c** in the ensemble of the three most divergent structures of ALR2 (sorbinil-, IDD594-, tolrestat-conformations). The docking program predicted that **5c** would be able to form a more stable complex with the IDD594 conformation with the best ranking conformation corresponding also to the most populated cluster ($\Delta G_{AD4} = -9.14$ kcal/mol, cluster size 60/100). On the other hand, in the sorbinil- and tolrestat-conformations the best ranking solutions do not belong to the most populated cluster (ΔG_{AD4} value of −7.27 kcal/mol and −7.61 kcal/mol, respectively). Visual inspection of the docking pose achieved in the most favored enzyme conformation (IDD594) revealed that compound **5c** would be unable to place its carboxylic moiety in proximity to the anion binding site and this holds true also for the other solutions achieved through docking calculations in the other enzyme conformations (sorbinil- and torlestat-conformations). In fact, the acidic group of the ligand establishes only two H-bonds interactions with W20 side-chain and with K21 backbone NH (Fig. 4) while the intrinsic rigidity of **5c** allows to

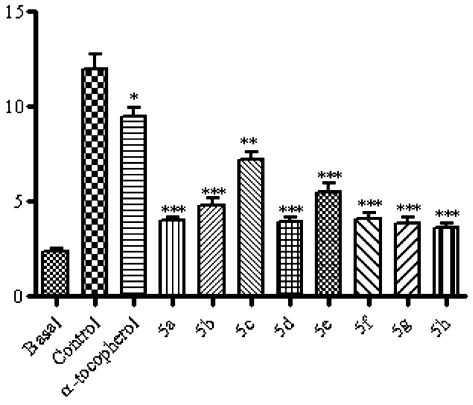

Fig. 2. Effects of 2,4-thiazolidinedione derivatives **5a**–**h** and α-tocopherol on the production of thiobarbituric reactive substances (TBARS) in rat brain homogenate, expressed as nmol of malondialdehyde (MDA)/10 mg of wet weight tissue. Each column represents the mean ± S.E.M. ($n = 6$). *, $p < 0.05$, significant difference versus control group (rat brain homogenate plus $FeCl_3$/ascorbic acid); **, $p < 0.01$, significant difference versus control group (rat brain homogenate plus $FeCl_3$/ascorbic acid); ***, $p < 0.001$, significant difference versus control group (rat brain homogenate plus $FeCl_3$/ascorbic acid).

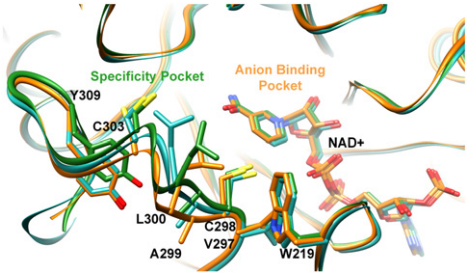

Fig. 3. ALR2 X-ray crystal structures induced by IDD594l (green), tolrestat (orange) and sorbinil (cyan). The most flexible residues in the specificity pocket are represented as sticks. (For interpretation of the references to colour in this figure legend, the reader is referred to the web version of this article.)

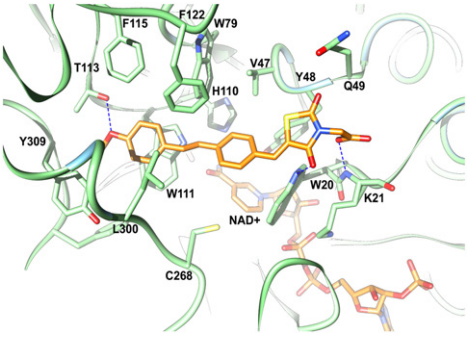

Fig. 4. Docked conformations of **5c** in the ALR2 structure. Hydrogens are omitted for clarity. Ligand carbon atoms are displayed in orange, and key binding site residues are displayed as green sticks. Hydrogen bonds are represented by dashed blue lines. (For interpretation of the references to colour in this figure legend, the reader is referred to the web version of this article.)

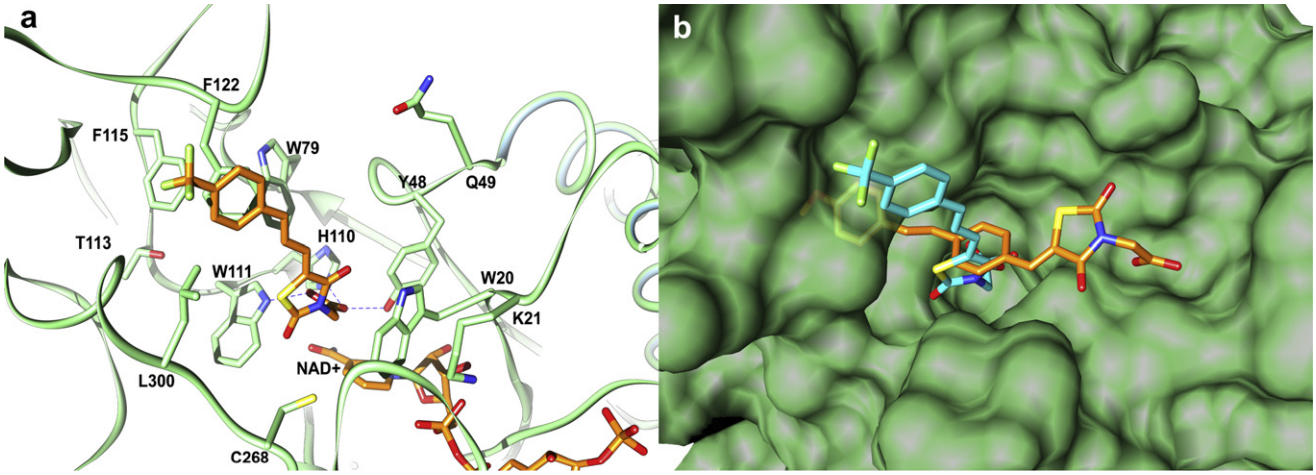

Fig. 5. (a) Docked conformations of **5h** in the ALR2 structure. Hydrogens are omitted for clarity. Ligand carbon atoms are displayed in orange, and key binding site residues are displayed as green sticks. Hydrogen bonds are represented by dashed blue lines. (b) Predicted binding orientations of **5c** (orange) and **5h** (cyan) in the ALR2 binding site depicted as green surface. (For interpretation of the references to colour in this figure legend, the reader is referred to the web version of this article.)

reach the specificity pocket where the terminal phenyl ring is engaged in a π-stacking interaction with W111 and the *p*-methoxy group establishes a H-bond with T113. In principle, this would explain why a detrimental effect was recorded with the substitution of the *p*-methoxy group with a *p*-trifluoromethyl one (**5d**) that would cause unfavorable interactions between the small electronegative crown of the fluorine atoms and the lone pair of T113 O^{γ} atom as already reported for other ARIs [23].

From the above considerations the binding pose achieved for **5c** would explain SARs data achieved for these ARIs, nevertheless the absence of any direct interaction with the enzyme anion site would cast some doubts on the reliability of the docking predictions. Actually, inspection of the numerous X-ray structures of this enzyme complexed with several ARIs reveals that the anion site is always contacted through polar interactions by the ligand carboxylate portion. Therefore, the unprecedented binding mode predicted for **5c** could be an artifactual result of the absence of a full protein flexibility during docking calculations.

To rationalize the opposite effects of the trifluoromethyl group on the ALR2 inhibitory activity of styrylbenzylidene (**5a**–**d**) and styrylmethylidene (**5e**–**h**) derivatives, we docked compound **5h** in the ALR2 binding site. Interestingly, more viable results were achieved. In fact, in the predicted binding pose (Fig. 5), showing a ΔG_{AD4} of −7.89 kcal/mol and a cluster size population of 57/100, the ligand is now able to take direct interaction with the anion binding pocket by means of H-bonding with W111, H110 and Y48. On the other hand, the terminal phenyl ring is now unable to interact with the specificity pocket while extending towards the vestibule of the enzyme active site. In such a position, the same ring is engaged in a π-π stacking interaction with the F122 side-chain. This might explain the higher inhibitory effectiveness of compound **5h**, which bears an electron-withdrawing substituent on the phenyl ring, in comparison with analogues **5e**–**g**.

4. Conclusions

The results of the present study indicate that 5-arylidene-2,4-thiazolidinediones **4**, **5** and 2-phenylimino analogues **8** inhibit ALR2. According to the SARs acquired for this class of compounds, acetic acids **5** are better inhibitors than N-unsubstituted derivatives **4**, reaching ALR2 inhibitory activity levels similar to that of epalrestat and more effective than sorbinil. Interestingly compounds **5** also exhibit excellent antioxidant properties. This additional feature could ameliorate their pharmacological profile as ALR2 inhibitors, since an increased quantity of ROS can be produced in the polyol pathway which worsens diabetes-induced tissue damage at different tissue levels. Compounds **5a** and **5h** are endowed with excellent ALR2 inhibition activity as well as being highly effectiveness as ROS scavenging molecules and are thus good candidates as dual target agents.

In our study, molecular modeling calculations allowed us to propose a hypothesis to explain in a qualitative manner the SAR data for the newly synthesized ARIs. Nevertheless, it should be pointed out that docking simulations for this set of inhibitors suggested at least for **5c** an unprecedented and may be artifactual binding pose in the ALR2 enzyme. Taking into account the high degree of plasticity of the specificity pocket upon inhibitor binding, only X-Ray crystallography studies will ultimately help to clarify the real binding position of this ARI.

5. Experimental section

5.1. Chemistry

Melting points were recorded on a Kofler hot-stage apparatus and are uncorrected. TLC controls were carried out on precoated silica gel plates (F 254 Merck). Elemental analyses (C, H, N), determined by means of a C. Erba mod. 1106 elem. Analyzer, were within ±0.4% of theory. ^{1}H and ^{13}C NMR spectra were recorded on a Varian 300 magnetic resonance spectrometer (300 MHz for ^{1}H and 75 MHz for ^{13}C). Chemical shifts are given in δ units (ppm) relative to internal standard Me_4Si and refer to DMSO-d_6 solutions. Coupling constants (J) are given in hertz (Hz). ^{13}C NMR spectra were determined by Attached Proton Test (APT) experiments and the resonances were always attributed by proton-carbon heteronuclear chemical shift correlation.

Unless stated otherwise, all materials were obtained from commercial suppliers and used without further purification.

(*E*)-4-(2-phenylethenyl)benzaldehyde (**3a**) and (*E*)-3-phenylpropenale (**3e**) were commercial samples of high purity grade (≥97%, Sigma Aldrich). The purity of synthetic compounds was established as ≥ 95% by elemental analysis and normal phase thin-layer chromatographic analysis.

Commercial aldehydes **3a** and **3e** are constituted by diastereomerically pure *E* isomers.

4-(2-Arylethenyl)benzaldehydes **3b**–**d** [24] and 3-aryl-2-propenales **3f**–**h** [25] were obtained via already reported procedures. In all cases both series of compounds **3b**–**d** and **3f**–**h** were obtained in *E* configuration as spectroscopic data indicated.

*5.1.1. General method for the synthesis of 4-(2-arylethenyl) benzaldehydes (**3b**–**d**)*

A mixture of NaCl (300 mg, 5.13 mmol) and montmorillonite-clay (25 g) in water (600 mL) was stirred for 24 h at room temperature. The suspension was decanted and washed with distilled water several times until the disappearance of chlorine ions and dried at 110 °C for 12 h. A suspension of the catalyst (6 g), $PdCl_2$ (300 mg, 1.73 mmol) and tetraphenylphosphonium bromide (1.5 g, 0.004 mmol) in H_2O (50 mL) was refluxed for 48 h. The solid obtained was filtered, washed with water and dried at 110 °C for 12 h.

A mixture of the previously obtained catalyst (200 mg), sodium acetate (1.71 g, 21.6 mmol), 4-bromobenzaldeide (2.0 g, 10.8 mmol) and the appropriate styrene (10.8 mmol) in DMF (25 mL) was refluxed for 3 h. The suspension was poured in water and the crude product was extracted with ethyl acetate. The organic solvent was evaporated in vacuo, and the product was purified by silica gel column chromatography (eluent diethyl ether/cyclohexane, 1/9).

*5.1.2. 4-[2-(4-Methylphenyl)ethenyl]benzaldehyde (**3b**)*

Yield: 83%; m.p. 139–141 °C; ^{1}H NMR (DMSO-d_6): δ 2.40 (s, 3H, CH_3), 7.10 (d J = 16.5 Hz, 1H, vinyl), 7.20–7.29 (m, 3H, arom and vinyl), 7.46 (m, 2H, arom), 7.65 (m, 2H, arom), 7.87 (m, 2H, arom), 10.01 (s, 1H, CHO). Anal. Calcd for $C_{16}H_{14}O$: C, 86.45; H, 6.35. Found C, 86.23; H, 5.99.

*5.1.3. 4-[2-(4-Methoxyphenyl)ethenyl]benzaldehyde (**3c**)*

Yield: 77%; yellow oil; ^{1}H NMR (DMSO-d_6): δ 3.85 (s, 3H, CH_3), 6.93 (m, 2H, arom); 7.01 (d J = 16.2 Hz, 1H, vinyl), 7.23 (d J = 16.4 Hz, 1H, vinyl), 7.49 (m, 2H, arom), 7.62 (m, 2H, arom), 7.85 (m, 2H, arom), 9.98 (s, 1H, CHO). Anal. Calcd for $C_{16}H_{14}O_2$: C, 80.65; H, 5.92. Found C, 80.44; H, 5.72.

*5.1.4. 4-[2-(4-Trifluoromethylphenyl)ethenyl]benzaldehyde (**3d**)*

Yield: 60%; m.p: 128–130 °C; ^{1}H NMR (DMSO-d_6): δ 7.53 (d J = 16.4 Hz, 1H, vinyl); 7.59 (d J = 16.4 Hz, 1H, vinyl), 7.76 (m, 2H, arom), 7.86 (m, 4H, arom), 7.93 (m, 2H, arom); 10.00 (s, 1H, CHO). Anal. Calcd for $C_{16}H_{11}F_3O$: C, 69.56; H, 4.01. Found C, 69.29; H, 3.98.

*5.1.5. General method for the synthesis of 3-aryl-2-propenales (**3f**–**h**)*

A mixture of the appropriate aryl bromide (0.5 mmol), acrolein diethyl acetate (0.229 mL, 1.5 mmol), ^{n}Bu$_4$NOAc (0.302 g, 1 mmol), K_2CO_3 (0.104 g, 0.75 mmol), KCl (0.037 g, 0.5 mmol) and $Pd(OAc)_2$ (0.003 g, 0.015 mmol) in DMF (30 mL) was stirred for 2 h at 90 °C. The mixture was cooled and HCl (2N) was added slowly and stirred for 10 min at room temperature. The reaction product was extracted with ethyl ether and then the organic layer was washed with water, dried over Na_2SO_4 and concentrated under reduced pressure. The product was purified by silica gel column chromatography (eluent diethyl ether/cyclohexane, 1/9).

*5.1.6. 3-(4-Methylphenyl)-2-propenale (**3f**)*

Yield: 60%; m.p. 43–45 °C; ^{1}H NMR ($CDCl_3$): δ 2.45 (s, 3H, CH_3), 6.73 (dd J = 16.2 Hz and J = 7.8 Hz, 1H, vinyl); 7.25 (m, 2H, arom); 7.31 (d J = 16.2 Hz, 1H, vinyl); 7.53 (m, 2H, arom); 9.76 (d J = 7.8 Hz, 1H, CHO). Anal. Calcd for $C_{10}H_{10}O$: C, 82.16; H, 6.89. Found C, 82.32; H, 6.58.

*5.1.7. 3-(4-Methoxyphenyl)-2-propenale (**3g**)*

Yield: 35%; m.p. 58–60 °C; ^{1}H NMR ($CDCl_3$): δ 3.87 (s, 3H, CH_3); 6.62 (dd J = 15.9 Hz and J = 7.8 Hz, 1H, vinyl); 6. 95 (m, 2H, arom); 7.43 (d J = 15.9 Hz, 1H, vinyl); 7.5 (m, 2H, arom); 9.66 (d J = 7.8 Hz, 1H, CHO). Anal. Calcd for $C_{10}H_{10}O_2$: C, 74.06; H, 6.21. Found C, 74.34; H, 6.32.

*5.1.8. 3-(4-Trifluoromethylphenyl)-2-propenale (**3h**)*

Yield: 70%; yellow oil; ^{1}H NMR ($CDCl_3$): δ 6.78 (dd J = 16.2 Hz and J = 7.8 Hz, 1H, 2–H); 7.54 (d J = 16.2 Hz, 1H, 3–H); 7.75 (m, 4H, arom); 9.76 (d J = 7.8 Hz, 1H, CHO). Anal. Calcd for $C_{10}H_7F_3O$: C, 60.01; H, 3.53. Found C, 60.22; H, 3.44.

*5.1.9. General method for the synthesis of 5-{[4-(2-arylethenyl) phenyl]methylidene}-2,4-thiazolidinediones (**4a-d**) and 5-(3-aryl-2-propen-1-ylidene)-2,4-thiazolidinediones (**4e**–**h**)*

A mixture of 2,4-thiazolidinedione (2.4 g, 20 mmol), appropriate aldehyde (20 mmol), piperidine (1.4 g, 16 mmol) in EtOH (100 mL) was refluxed for 24 h. The reaction mixture was poured into H_2O and acidified with glacial AcOH until pH 3–4 to give a crude solid. The product was crystallized from methanol providing pure compounds **4**.

*5.1.10. 5-{[4-(2-Phenylethenyl)phenyl]methylidene}-2,4-thiazolidinedione (**4a**)*

Yield 48%; mp 270–273 °C; ^{1}H NMR ($CDCl_3$): δ 7.28–7.44 (m, 5 H, arom and vinyl), 7.58–7.64 (m, 4H, arom), 7.75 (m, 2H, arom). 7.78 (s, 1H, CH methylidene); ^{13}C NMR ($CDCl_3$): δ 127.2, 127.8 (vinyl); 127.6, 128.6, 129.2, 130.9, 131.1 (CH arom); 131.7 (CH methylidene); 123.4 (5–C); 132.5, 137.1, 139.5 (Cq arom); 167.9, 168.3 (CO). Anal. Calcd. for $C_{18}H_{13}NO_2S$: C, 70.34; H, 4.26; N, 4.56. Found C, 70.69; H, 4.57; N, 4.76.

*5.1.11. 5-({[4-[2-(4-Methylphenyl)ethenyl]phenyl}methylidene)-2,4-thiazolidinedione (**4b**)*

Yield 43%; mp 260–262 °C; ^{1}H NMR (DMSO-d_6): δ 2.26 (s, 3H, CH_3); 6.96 (d J = 16.5 Hz, 1H, vinyl); 7.07 (m, 3H, arom and vinyl); 7.32–7.39 (m, 4H, arom); 7.49 (m, 2H, arom); 7.65 (s, 1H, CH methylidene); ^{13}C NMR (DMSO-d_6): δ 21.3 (CH_3); 126.8, 131.5 (vinyl); 127.2, 127.5, 129.8, 131.0 (CH arom); 131.8 (CH methylidene); 123.2 (5–C); 132.3, 134.4, 138.1, 139.8 (Cq arom); 167.8, 168.3 (CO). Anal. Calcd. for $C_{19}H_{15}NO_2S$: C, 71.0; H, 4.70; N, 4.36. Found C, 71.32; H, 3.99; N, 4.32.

*5.1.12. 5-({[4-[2-(4-Methoxyphenyl)ethenyl]phenyl}methylidene)-2,4-thiazolidinedione (**4c**)*

Yield 55%; mp 268–270 °C; ^{1}H NMR (DMSO-d_6): δ 3.78 (s, 3H, CH_3); 6.97 (m, 2H arom); 7.15 (d J = 16.5 Hz, 1H, vinyl); 7.35 (d J = 16.5 Hz, 1H, vinyl); 7.58 (m, 4H, arom); 7.72 (m, 2H, arom); 7.77 (s, 1H, CH methylidene); ^{13}C NMR (DMSO-d_6): δ 55.5 (CH_3); 125.4, 126.2 (vinyl); 114.7, 127.3, 128.7, 131.0 (CH arom); 131.9 (CH methylidene); 123.0 (5–C); 129.8, 132.0, 140.1, 159.9 (Cq arom); 167.8, 168.2 (CO). Anal. Calcd. for $C_{19}H_{15}NO_3S$: C, 67.64; H, 4.48; N, 4.15. Found C, 67.33; H, 4.22; N, 4.35.

*5.1.13. 5-({[4-[2-(4-Trifluoromethylphenyl)ethenyl]phenyl} methylidene)-2,4-thiazolidinedione (**4d**)*

Yield 41%; mp 224–226 °C; ^{1}H NMR (DMSO-d_6): δ 7.27–7.45 (m, 4H, arom and vinyl); 7.59 (m, 2H, arom); 7.70–7.83 (m, 5H, arom and CH methylidene); ^{13}C NMR (DMSO-d_6): δ 126.9, 127.4, (vinyl); 125.0, 126.3, 126.7, 131.2 (CH arom); 122.8 (5–C); 132.5 (CH methylidene); 124.2 (CF_3 J_{CF} = 270.1 Hz); 130.2, 134.4, 138.5, 140.1 (Cq arom); 166.3, 167.1 (CO). Anal. Calcd. for $C_{19}H_{12}F_3NO_2S$: C, 60.80; H, 3.22; N, 3.73. Found C, 60.52; H, 3.45; N, 3.92.

*5.1.14. 5-(3-Phenyl-2-propen-1-ylidene)-2,4-thiazolidinedione (**4e**)*

Yield 50%; mp 195–197 °C; ^{1}H NMR (DMSO-d_6): δ 6.90 (dd J = 11.4 Hz and J = 15.3 Hz, 1H, vinyl); 7.26 (d J = 15.3 Hz, 1H, vinyl); 7.36–7.41 (m, 3H, arom), 7.46 (d J = 11.4 Hz, 1H, CH methylidene); 7.63–7.65 (m, 2H, arom); 12.40 (brs, 1H, NH exchangeable with D_2O); ^{13}C NMR (DMSO-d_6): δ 123.8, 143.7 (vinyl), 128.1 (CH methylidene); 129.3, 130.1, 132.5 (CH arom); 125.3 (5–C); 135.9 (Cq arom); 167.1, 168.0 (CO). Anal. Calcd. for $C_{12}H_9NO_2S$: C, 62.32; H, 3.92; N, 6.06. Found C, 62.14; H, 3.64; N, 5.89.

*5.1.15. 5-[3-(4-Methylphenyl)-2-propen-1-ylidene]-2,4-thiazolidinedione (**4f**)*

Yield 43%; mp 170–172 °C; ^{1}H NMR (DMSO-d_6): δ 2.31 (s, 3H, CH_3); 6.85 (dd J = 11.1 Hz and J = 15.0 Hz, 1H, vinyl); 7.21 (m, 2H, arom); 7.23 (d J = 15.0 Hz, 1H, vinyl); 7.46 (d J = 11.4 Hz, 1H, CH methylidene); 7.55 (m, 2H, arom); 12.36 (brs, 1H, NH exchangeable with D_2O); ^{13}C NMR (DMSO-d_6): δ 21.43 (CH_3); 122.8, 143.9 (vinyl); 128.2, 129.9 (CH arom); 132.7 (CH methylidene); 124.5 (5–C); 133.3, 140.0 (Cq arom); 167.1, 168.0 (CO). Anal. Calcd. for $C_{13}H_{11}NO_2S$: C, 63.65; H, 4.52; N, 5.71. Found C, 61.44; H, 4.31; N, 5.89.

*5.1.16. 5-[3-(4-Methoxyphenyl)-2-propen-1-ylidene]-2,4-thiazolidinedione (**4g**)*

Yield 43%; mp 190–192 °C; ^{1}H NMR (DMSO-d_6): δ 3.80 (s, 3H, CH_3); 6.77 (dd J = 11.4 Hz and J = 15.0 Hz, 1H, vinyl); 6.98 (m, 2H, arom); 7.24 (d J = 15.0 Hz, 1H, vinyl); 7.46 (d J = 11.4 Hz, 1H, CH methylidene); 7.63 (m, 2H, arom); 12.38 (brs, 1H, NH exchangeable with D_2O). ^{13}C NMR (DMSO-d_6): δ 55.8 (CH_3); 125.2, 141.3 (CH vinyl); 114.2, 127.4 (CH arom); 123.9 (5–C); 131.6 (CH methylidene); 127.5, 159.8 (Cq arom); 166.5, 167.3 (CO). Anal. Calcd for $C_{13}H_{11}NO_3S$: C, 59.76; H, 4.24; N, 5.36. Found C, 57.26; H, 4.11; N, 5.08.

*5.1.17. 5-[3-(4-Trifluoromethylphenyl)-2-propen-1-ylidene]-2,4-thiazolidinedione (**4h**)*

Yield 43%; mp 218–220 °C; ^{1}H NMR (DMSO-d_6): δ 7.12 (dd J = 11.4 Hz and J = 15.0 Hz, 1H, vinyl); 7.38 (d J = 15.0 Hz, 1H, vinyl); 7.52 (d J = 11.4 Hz, 1H, CH methylidene); 7.76 (m, 2H, arom); 7.91 (m, 2H, arom); 12.50 (brs, 1H, NH); ^{13}C NMR (DMSO-d_6): δ 126.5, 141.6 (vinyl); 131.7 (CH methylidene); 126.1, 128.8 (CH arom); 127.2 (5–C); 139.9 (Cq arom), 129.7 (C-CF_3 J_{CF} = 33.0 Hz), 124.6 (CF_3 J_{CF} = 270.0 Hz); 167.2, 168.0 (CO). Anal. Calcd for $C_{13}H_8F_3NO_2S$: C, 52.17; H, 2.69; N, 4.68. Found C, 52.42; H, 2.72; N, 4.44.

*5.1.18. General method for the synthesis of [5-{[4-(2-arylethenyl) phenyl]methylidene}-2,4-dioxothiazolidin-3-yl]acetic acids (**5a**–**d**) and {2,4-dioxo-5-[3-phenyl-2-propen-1-ylidene]thiazolidin-3-yl} acetic acids (**5e**–**h**)*

A mixture of **4** (10 mmol), methyl bromoacetate (6.12 g, 40 mmol) and potassium carbonate (5.53 g, 40 mmol) in acetone (150 mL) was refluxed for 24 h. The solvent was evaporated under reduced pressure. The solid residue was washed with H_2O and then refluxed in glacial AcOH (40 mL) and HCl 12N (10 mL) for 2 h. After evaporation in vacuo, the residue was refluxed again with AcOH (40 mL) and HCl (10 mL) for 2 h. After evaporation in vacuo, the crude solid was washed with H_2O and crystallized from ethanol providing pure carboxylic acids **5**.

*5.1.19. [2,4-Dioxo-5-{[4-(2-phenylethenyl)phenyl]methylidene} thiazolidin-3-yl]acetic acid (**5a**)*

Yield 90%; mp 256–258 °C; ^{1}H NMR (DMSO-d_6): δ 4.38 (s, 2H, CH_2); 7.29–7.79 (m, 11H, arom and vinyl); 7.98 (s, 1H, CH methylidene); ^{13}C NMR (DMSO-d_6): δ 45.5 (CH_2); 127.1, 127.5 (vinyl); 126.4, 127.9, 128.0, 128.7, 131.3 (CH arom); 121.1 (5–C); 133.1 (CH methylidene); 135.2, 134.4, 138.2 (Cq arom); 164.4, 167.6, 169.8 (CO). Anal. Calcd for $C_{20}H_{15}NO_4S$: C, 65.74; H, 4.14; N, 3.83. Found C, 65.99; H, 3.89; N, 4.01.

*5.1.20. [5-({4-[2-(4-Methylphenyl)ethenyl]phenyl}methylidene)-2,4-dioxothiazolidin-3-yl]acetic acid (**5b**)*

Yield 95%; mp 265–268 °C; ^{1}H NMR (DMSO-d_6): δ 2.30 (s, 3H, CH_3); 4.37 (s, 2H, CH_2); 7.20 (m, 2H, arom); 7.24 (d J = 16.5 Hz, 1H, vinyl); 7.38 (d J = 16.5 Hz, 1H, vinyl); 7.51 (m, 2H, arom); 7.63 (m, 2H, arom); 7.74 (m, 2H, arom); 7.96 (s, 1H, CH methylidene); ^{13}C NMR (DMSO-d_6): δ 21.3 (CH_3); 45.8 (CH_2); 126.8, 131.4 (vinyl); 127.2, 127.6, 129.9, 131.2 (CH arom); 133.9 (CH methylidene); 120.9 (5–C); 132.0, 134.4, 138.2, 140.3 (Cq arom); 165.4, 167.2, 168.4 (CO). Anal. Calcd for $C_{21}H_{17}NO_4S$: C, 66.47; H, 4.52; N, 3.69. Found C, 65.98; H, 4.33; N, 3.84.

*5.1.21. [5-({4-[2-(4-Methoxyphenyl)ethenyl]phenyl}methylidene)-2,4-dioxothiazolidin-3-yl]acetic acid (**5c**)*

Yield 98%; mp 262–265 °C; ^{1}H NMR (DMSO-d_6): δ 3.77 (s, 3H, CH_3); 4.38 (s, 2H, CH_2); 6.97 (m, 2H, CH arom); 7.15 (d J = 16.5 Hz, 1H, vinyl); 7.38 (d J = 16.5 Hz, 1H, vinyl); 7.57–7.65 (m, 4H, arom); 7.73 (d, 2H, arom); 7.97 (s, 1H, CH methylidene); ^{13}C NMR (DMSO-d_6): δ 42.6 (CH_2); 55.6 (OCH_3); 125.4, 133.9 (vinyl); 114.6, 127.3, 128.5, 131.2 (CH arom); 133.9 (CH methylidene); 120.0 (5–C); 129.6, 131.6, 140.5, 159.9 (Cq arom); 162.2, 167.2, 168.3 (CO). Anal. Calcd for $C_{21}H_{17}NO_5S$: C, 63.79, H, 4.33; N, 3.54. Found C, 63.45, H, 4.54; N, 3.41.

*5.1.22. [5-({4-[2-(4-Trifluoromethylphenyl)ethenyl]phenyl} methylidene)-2,4-dioxothiazolidin-3-yl]acetic acid (**5d**)*

Yield 93%; mp 255–256 °C; ^{1}H NMR (DMSO-d_6): δ 4.39 (s, 2H, CH_2); 7.50 (s, 2H, vinyl); 7.68 (m, 2H, arom); 7.80–7.86 (m, 4H, arom); 7.99 (s, 1H, CH methylidene). ^{13}C NMR (DMSO-d_6): δ 45.4 (CH_2); 127.4, 132.5 (vinyl); 125.6, 126.5, 126.9, 130.8 (CH arom); 121.3 (5–C); 133.6 (CH methylidene); 124.8 (CF_3 J_{CF} = 270.3 Hz); 130.5, 134.6, 138.2, 140.3 (Cq arom); 164.4, 176.8, 173.1 (CO). Anal. Calcd for $C_{21}H_{14}F_3NO_4S$: C, 58.20; H, 3.26; N, 3.23. Found C, 58.44; H, 2.99; N, 3.55.

*5.1.23. [2,4-dioxo-5-(3-phenyl-2-propen-1-ylidene)thiazolidin-3-yl]acetic acid (**5e**)*

Yield 93%; mp 215–217 °C; ^{1}H NMR (DMSO-d_6): δ 4.33 (s, 2H, CH_2); 7.03 (dd J = 11.7 Hz and J = 15.6 Hz, 1H, vinyl); 7.35–7.41 (m, 4H, arom and vinyl); 7.66–7.70 (m, 3H, arom and CH methylidene); ^{13}C NMR (DMSO-d_6): δ 41.2 (CH_2); 122.0, 142.0 (vinyl); 121.5 (5–C); 126.4 (CH methylidene); 127.2, 129.4, 130.3 (CH arom); 139.9 (Cq arom); 165.0, 167.1, 168.0 (CO). Anal. Calcd for $C_{14}H_{11}NO_4S$: C, 58.12; H, 3.83; N, 4.84. Found C, 57.99; H, 3.63; N, 4.73.

*5.1.24. {5-[3-(4-Methylphenyl)-2-propen-1-ylidene]-2,4-dioxothiazolidin-3-yl}acetic acid (**5f**)*

Yield 93%; mp 190–193 °C; ^{1}H NMR (DMSO-d_6): δ 2.32 (s, 3H, CH_3); 4.33 (s, 2H, CH_2); 6.96 (dd J = 11.4 Hz and J = 15.3 Hz, 1H, vinyl); 7.23 (m, 2H, arom); 7.34 (d J = 15.3 Hz, 1H, vinyl); 7.58 (m, 2H, arom); 7.67 (d J = 11.4 Hz, 1H, CH methylidene); ^{13}C NMR (DMSO-d_6): δ 21.5 (CH_3); 42.6 (CH_2); 122.6, 145.3 (vinyl); 121.4 (5–C); 134.9 (CH methylidene); 128.4, 130.0 (CH arom); 133.2, 140.5 (Cq arom); 164.9, 167.1, 168.3 (CO). Anal. Calcd for $C_{15}H_{13}NO_4S$: C, 59.39; H, 4.32; N, 4.62. Found C, 59.11; H, 4.12; N, 4.44.

*5.1.25. {5-[3-(4-Methoxyphenyl)-2-propen-1-ylidene]-2,4-dioxothiazolidin-3-yl}acetic acid (**5g**)*

Yield 95%; mp 205–207 °C; ^{1}H NMR (DMSO-d_6): δ 3.80 (s, 3H, CH_3); 4.32 (s, 2H, CH_2); 6.87 (dd J = 11.4 Hz and J = 15.0 Hz, 1H, vinyl); 6.97 (m, 2H, arom); 7.32 (d J = 15.3 Hz, 1H, vinyl); 7.60–7.66 (m, 3H, arom and CH methylidene); ^{13}C NMR (DMSO-d_6): δ 42.9 (CH_2); 55.7 (CH_3); 121.4, 145.3 (vinyl); 120.4 (5–C); 135.3 (CH

methylidene); 115.0, 130.4 (CH arom); 128.7, 152.6 (Cq arom); 161.5, 167.3, 168.4 (CO). Anal. Calcd for $C_{15}H_{13}NO_5S$: C, 56.42, H, 4.1; N, 4.39. Found C, 56.29, H, 3.89; N, 4.25.

*5.1.26. {5-[3-(4-Trifluoromethylphenyl)-2-propen-1-ylidene]-2,4-dioxothiazolidin-3-yl}acetic acid (**5h**)*

Yield 97%; mp 200–203 °C; ^{1}H NMR (DMSO-d_6): δ 4.34 (s, 2H, CH_2); 7.20 (dd J = 11.4 Hz and J = 15.0 Hz, 1H, vinyl); 7.43 (d J = 15.0 Hz, 1H, vinyl); 7.68 (d J = 11.4 Hz, 1H, CH methylidene); 7.75 (m, 2H, arom); 7.90 (m, 2H, arom); ^{13}C NMR (DMSO-d_6): δ 42.8 (CH_2); 126.1, 142.9 (vinyl); 124.1 (5–C); 124.2 (CF_3 J_{CF} = 270.3 Hz); 130.1 (C-CF_3 J_{CF} = 17.0 Hz); 133.9 (CH methylidene); 126.2, 128.9 (CH arom); 139.9 (Cq arom); 165.0, 167.0, 168.5 (CO). Anal. Calcd for $C_{15}H_{10}F_3NO_4S$: C, 50.42, H, 2.82; N, 3.92. Found C, 50.14, H, 2.55; N, 3.78.

*5.1.27. Synthesis of 2-[(phenylcarbamothioyl)amino]acetic acid (**6**)*

A hydroalcoholic mixture of phenylisothiocyanate (0.35 g, 2.6 mmol), 2-aminoacetic acid (0.5 g, 3.3 mmol) and K_2CO_3 (5.5 g, 40 mmol) was refluxed for 24 h. The solvent was evaporated under vacuo and the solid residue was dissolved in water and HCl concentrated was added drop by drop up to complete elimination of K_2CO_3. The organic layer was washed and dried with Na_2SO_4; the solvent was evaporated in vacuo and the crude solid was crystallized from methanol providing compound **6**.

Yield 74%; mp 139–141 °C; ^{1}H NMR (DMSO-d_6): δ 4.19 (d J = 5.7 Hz, 2H, CH_2); 7.09–7.14 (m, 1H, arom); 7.29–7.35 (m, 2H, arom); 7.40–7.43 (m, 2H, arom), 7.84 (t J = 5.7 Hz, 1H, CH_2NH); 9.86 (brs exchangeable with D_2O, 1H, NH); 11.05 (brs, 1H, COOH); ^{13}C NMR (DMSO-d_6): δ 46.3 (CH_2); 123.8, 125.1, 129.5 (CH arom); 139.5 (Cq arom); 171.7 (C=O); 181.5 (C=S); Anal. calcd for $C_9H_{10}N_2O_2S$: C, 51.41; H, 4.79; N, 13.32. Found: C, 51.33; H, 4.71; N, 9.98.

*5.1.28. Synthesis of 2-(4-oxo-2-phenyliminothiazolidin-3-yl)acetic acid (**7**)*

A mixture of **6** (1.2 g, 5.8 mmol), triethylamine (1.7 g, 17.4 mmol) and chloroacetic chloride (0.9 g, 8.7 mmol) in ethanol (50 mL) was maintained at reflux for 24 h. After evaporation of the solvent under reduced pressure, the crude solid was dissolved in $CHCl_3$. The organic solution was washed with water and then acidified with HCl. The evaporation of the solvent under reduced pressure and crystallization from methanol provided pure compound **7**.

Yield 62%; yellow oil; ^{1}H NMR ($CDCl_3$): δ 3.91 (s, 2H, 5–CH_2); 4.66 (s, 2H, NCH_2); 6.98 (m, 2H, arom); 7.17 (m, 1H, arom); 7.32–7.38 (m, 2H, arom); ^{13}C NMR ($CDCl_3$): δ 32.4 (5–CH_2); 43.1 (NCH_2); 120.8, 124.6, 128.9 (CH arom); 146.9 (Cq arom); 153.8 (C=N); 169.7, 171.7 (C=O); Anal. calcd for $C_{11}H_{10}N_2O_3S$: C, 52.79; H, 4.03; N 11.19. Found: C, 52.68; H, 4.17; N, 10.89.

*5.1.29. General method for the synthesis of (5-arylidene-4-oxo-2-phenyliminothiazolidin-3-yl)acetic acids (**8i–k**)*

A mixture of acid **7** (0.7 g, 2.7 mmol), appropriate aldehyde (2.7 mmol) and piperidine (0.4 g, 4.32 mmol) in ethanol (5 mL) was treated by irradiation with microwaves for 6 h. The solution was poured in water acidified with glacial acetic (pH 3-4); the crude solid was washed with H_2O and recrystallized from methanol providing pure acids **8**.

*5.1.30. [4-oxo-5-(4-phenoxyphenylmethylidene)-2-phenyliminothiazolidin-3-yl]acetic acid (**8i**)*

Yield 37%; mp 176–179 °C; ^{1}H NMR ($CDCl_3$): δ 4.81 (s, 2H, CH_2); 6.99–7.43 (m, 14H, arom); 7.76 (s, 1H, CH); ^{13}C NMR ($CDCl_3$): δ 43.4 (NCH_2); 118.3, 119.9, 121.4, 124.4, 125.3, 129.4, 130.0, 131.7 (CH arom); 131.9 (CH methylidene); 119.0 (5–C); 127.9, 147.0, 155.6, 159.4, 159.6 (Cq arom); 150.6 (C=N); 166.3, 171.3 (C=O); Anal. calcd for $C_{24}H_{18}N_2O_4S$: C, 66.96; H, 4.21; N 6.51. Found: 66.86; H, 4.31; N 6.47.

*5.1.31. [5-(4-Benzyloxyphenylmethylidene)-4-oxo-2-phenyliminothiazolidin-3-yl]acetic acid (**8j**)*

Yield 31%; mp 224–226 °C; ^{1}H NMR ($CDCl_3$): δ 4.55 (s, 2H, N-CH_2); 5.01 (s, 2H, OCH_2); 6.87–7.34 (m, 14H, arom); 7.61 (s, 1H, CH); ^{13}C NMR ($CDCl_3$): δ 43.5 (NCH_2); 69.9 (OCH_2); 115.4, 121.0, 124.8, 127.5, 128.0, 128.5, 129.2, 130.9 (CH arom); 131.8 (CH methylidene); 118.3 (5–C); 149.7 (C=N); 126.2, 136.2, 147.6, 147.7, 157.6 (Cq arom); 166.0, 166.1 (C=O); Anal. calcd for $C_{25}H_{20}N_2O_4S$: C, 67.55; H, 4.54; N 6.30. Found: 67.39; H, 4.31; N 6.44.

*5.1.32. [5-(Naphtalen-2-ylmethylidene)-4-oxo-2-phenyliminothiazolidin-3-yl]acetic acid (**8k**)*

Yield 46%; mp 238–240 °C; ^{1}H NMR ($CDCl_3$): δ 4.66 (s, 2H, CH_2); 6.96 (m, 2H, arom); 7.13 (m, 1H, arom); 7.31–7.49 (m, 6H, arom); 7.76–7.79 (m, 3H, arom), 7.86 (s, 1H, CH); ^{13}C NMR ($CDCl_3$): δ 43.4 (NCH_2); 120.9, 124.7, 125.7, 126.6, 127.4, 128.3, 128.5, 129.1, 130.4, 130.5, 131.1, 131.2 (CH arom); 121.2 (5–C); 130.8 (CH methylidene); 132.8, 133.2, 147.4 (Cq arom); 149.4 (C=N); 168.5, 166.0 (2 C=O); Anal. calcd for $C_{22}H_{16}N_2O_3S$: C, 68.20; H, 4.15; N 7.21. Found: C, 68.39; H, 4.07; N, 6.99.

5.2. Aldose reductase inhibition assay

Calf eyes were obtained from a local abattoir soon after slaughtering; lenses were removed and kept frozen at −20 °C until used. Aldose reductase was purified from bovine lens by a ionic exchange chromatographic step on DE-52 and an affinity chromatographic step on Matrex Orange A [26]. The final enzyme preparation (0.8 U/mg specific activity) was stored at 4 °C in 10 mM sodium phosphate buffer pH 7.0 supplemented with 2 mM dithiothreitol.

The enzyme activity was measured at 37 °C, using 4.67 mM D, L-glyceraldehyde as substrate in 0.25 M sodium phosphate, pH 6.8, 0.38 M ammonium sulfate, 0.11 mM NADPH, and 0.5 mM EDTA. One Unit of enzyme activity is the amount of enzyme that catalyzes the oxidation of 1 μmol/min of NADPH in the above assay conditions.

The sensitivity of aldose reductase to different compounds was tested in the above assay conditions in the presence of inhibitors dissolved at proper concentration in DMSO. The concentration of DMSO in the assay mixture was kept constant at 1% (v/v). IC_{50} values (the concentration of the inhibitor required to produce a 50% inhibition of the enzyme catalyzed reaction) were determined by non linear regression analysis by fitting the data to the equation describing one site competition in a log dose-inhibition curve. Each log dose-inhibition curve was generated using at least seven concentrations of inhibitor causing an inhibition between 10 and 90. The 95% confidence limits (95% CL) were calculated using GraphPad Prism software.

5.3. Thiobarbituric acid reagent substance (TBARS) assay

Freshly isolated rat brain was homogenised in 10% (w/v) phosphate buffer, pH 7.4. 20 μM $FeCl_3$ and 100 μM ascorbic acid (final concentrations) were added to 100 μL of rat brain homogenate, in the absence or presence of the test compound or the reference α-tocopherol, and were diluted till 1 mL with phosphate buffer, pH 7.4. Samples were incubated for 30 min at 37 °C in a water bath under slight stirring, and were then mixed with 0.5 mL of thiobarbituric acid (1% w/v in 0.05 N NaOH) and 0.5 mL 25% v/v HCl. The mixture was boiled for 10 min and, after cooling in an ice-cold water bath, extraction was performed with 3 mL of *n*-butanol. After liquid phase separation (centrifugation at 2000 g for 10 min), the absorbance of the pink organic phase was spectrophotometrically evaluated at 532 nm and TBARS was expressed as nmoles of malondialdehyde (MDA)/10 mg of rat brain tissue (wet weight). Absolute values were calculated by performing for each experiment a reference curve using 1,1,3,3-tetramethoxypropane as the standard reference.

Results are given as mean ± S.E.M., and are obtained through at least two different determinations performed in triplicate. The statistical significance of data was evaluated by unpaired *t*-test using Prism 4.0 software (GraphPad, San Diego, CA) [27].

5.4. Computational chemistry. AD4 docking calculations

The new version of the docking program AutoDock (version 4, AD4) [21], which already proved to be particularly suitable for an "ensemble docking" approach [28], as implemented through the graphical user interface called AutoDockTools (ADT), was used to dock **5c** and **5h**. The constructed compounds and receptor structure were converted to AD4 format files using ADT generating automatically all other atom values. The docking area was visually centered at the center of the anion binding site. A set of grids of 60 Å × 60 Å × 60 Å with 0.375 Å spacing was calculated around the docking area for the ligand atom types using AutoGrid4. For each ligand, 100 separate docking calculations were performed. Each docking calculation consisted of 10 million energy evaluations using the Lamarckian genetic algorithm local search (GALS) method. The GALS method evaluates a population of possible docking solutions and propagates the most successful individuals from each generation into the subsequent generation of possible solutions. A low-frequency local search according to the method of Solis and Wets is applied to docking trials to ensure that the final solution represents a local minimum. All dockings described in this paper were performed with a population size of 250, and 300 rounds of Solis and Wets local search were applied with a probability of 0.06. A mutation rate of 0.02 and a crossover rate of 0.8 were used to generate new docking trials for subsequent generations, and the best individual from each generation was propagated over the next generation. The docking results from each of the 100 calculations were clustered on the basis of root-mean square deviation (rmsd) (solutions differing by less than 2.0 Å) between the Cartesian coordinates of the atoms and were ranked on the basis of free energy of binding (ΔG_{AD4}). The top-ranked compounds were visually inspected for good chemical geometry. Calculated binding poses were rendered using the UCSF Chimera software [29].

Acknowledgments

This work was supported by University of Messina and University of Pisa.

References

[1] S. Wild, G. Roglic, A. Green, R. Sicree, H. King, Diabetes Care 27 (2004) 1047–1053.
[2] P.F. Kador, Med. Res. Rev. 8 (1998) 325–352.
[3] a) The diabetes control and complications trial research group. The effect of intensive treatment of diabetes on the development and progression of long-term complications in insulin-dependent diabetes mellitus, N. Engl. J. Med. 339 (1993) 977–986;
b) UK Prospective Diabetes Study (UKPDS) Group, Intensive blood-glucose control with sulphonylureas or insulin compared with conventional treatment and risk of complications in patients with type 2 diabetes (UKPDS 33), The Lancet 352 (1998) 837–853.
[4] L. Costantino, G. Rastelli, M.C. Gamberini, D. Barlocco, Exp. Opin. Ther. Patents 10 (2000) 1245–1262.
[5] M. Brownlee, Diabetes 54 (2005) 1615–1625.
[6] S.M. Son, Diabetes Res. Clin. Pract. 77 (2007) S65–S70.
[7] D. Jay, H. Hitomi, K.K. Griendling, Free Radic. Biol. Med. 40 (2006) 183–192.
[8] S.D. Yan, A.M. Schmidt, G.M. Anderso, J. Zang, J. Brett, Y.S. Zou, D. Pinsky, D. Stern, J. Biol. Chem. 269 (1994) 9889–9897.
[9] H. Kusunoki, S. Miyata, T. Ohara, B.F. Liu, A. Uriuhara, H. Kojima, K. Suzuki, H. Miyazaki, Y. Yamashita, K. Inaba, M. Kasuga, Diabetes Care 26 (2003) 1889–1894.
[10] C. Yabe-Nishimura, Pharmacol. Rev. 50 (1998) 21–34.
[11] S.K. Srivastava, K.V. Ramana, A. Bhatnagar, Endocr. Rev. 226 (2005) 380–392.
[12] K.V. Ramana, S.K. Srivastava, Int. J. Biochem. Cell Biol. 42 (2010) 17–20.
[13] a) P. Alexiou, K. Pegklidou, M. Chatzopoulou, I. Nicolaou, V.J. Demopoulos, Curr. Med. Chem. 16 (2009) 734–752;
b) R. Maccari, R. Ottanà, 2,4-Thiazolidinedione and 2-thioxo-4-thiazolidinone derivatives as aldose reductase inhibitors in the search for drugs to prevent long-term diabetes complications. in: M. Stefek (Ed.), Advances in Molecular Mechanisms and Pharmacology of Diabetic Complications. Transworld Research Network, Kerala, 2010, pp. 219–245.
[14] a) C.A. Sotriffer, O. Krämer, G. Klebe, Proteins 56 (2004) 52–66;
b) M. Zentgraf, H. Steuber, C. Koch, C. La Motta, S. Sartini, C.A. Sotriffer, G. Klebe, Angew. Chem. Int. Ed. 46 (2007) 3575–3578.
[15] a) R. Maccari, R. Ottanà, C. Curinga, M.G. Vigorita, D. Rakowitz, T. Steindl, T. Langer, Bioorg. Med. Chem. 13 (2005) 2809–2823;
b) R. Maccari, R. Ottanà, R. Ciurleo, M.G. Vigorita, D. Rakowitz, T. Steindl, T. Langer, Bioorg. Med. Chem. Lett. 17 (2007) 3886–3893;
c) R. Maccari, R. Ottanà, R. Ciurleo, D. Rakowitz, B. Matuszczak, C. Laggner, T. Langer, Bioorg. Med. Chem. 16 (2008) 5840–5852;
d) R. Maccari, R. Ciurleo, M. Giglio, M. Cappiello, R. Moschini, A. Del Corso, U. Mura, R. Ottanà, Bioorg. Med. Chem. 18 (2010) 4049–4055.
[16] S. Ostergaard, H.B. Olsen, N.C. Kaarsholm, P. Madsen, P. Jakobsen, S. Ludvigsen, G. Schluckebier, D. Steensgaard, A.K. Petersen, PCT Int. Appl (2004) WO 2004080480 A1 20040923.
[17] D.H. Yang, B.Y. Yang, Z.C. Chen, S.Y. Chen, Org. Prep. Proc. Int. 38 (2006) 81–85.
[18] A. Sugimoto, M. Shinichi, T. Morizo, U. Taro, Jpn. Kokai Tokkyo Koho (1996) JP 08109174 A.
[19] R. Ottanà, R. Maccari, M.L. Barreca, G. Bruno, A. Rotondo, A. Rossi, G. Chiricosta, R. Di Paola, L. Saubetin, S. Cuzzocrea, M.G. Vigorita, Bioorg. Med. Chem. 13 (2005) 4243–4252.
[20] G.W. Burton, K.U. Ingold, Ann. N. Y. Acad. Sci. 570 (1989) 7–22.
[21] R. Huey, G.M. Morris, A.J. Olson, D.S. Goodsell, J. Comput. Chem. 28 (2007) 1145–1152.
[22] S. Cosconati, L. Marinelli, C. La Motta, S. Sartini, F. Da Settimo, A.J. Olson, E. Novellino, J. Med. Chem. 52 (2009) 5578–5581.
[23] C. La Motta, S. Sartini, S. Salerno, F. Simorini, S. Taliani, A.M. Marini, F. Da Settimo, L. Marinelli, V. Limongelli, E. Novellino, J. Med. Chem. 51 (2008) 3182–3193.
[24] R.S. Varma, K.P. Naicker, P.J. Liesen, Tetrahedron Lett. 40 (1999) 2075–2078.
[25] G. Battistuzzi, S. Cacchi, G. Fabrizi, Org. Lett. 5 (2003) 777–780.
[26] A. Del Corso, D. Barsacchi, M. Giannessi, M.G. Tozzi, M. Camici, J.L. Houben, M. Zandomeneghi, U. Mura, Arch. Biochem. Biophys. 283 (1990) 512–518.
[27] M. Cantore, S. Siano, M. Coronnello, L. Mazzetti, S. Franchi-Micheli, M. Ciuffi, P. Failli, J. Photochem. Photobiol. B. 75 (2005) 34–42.
[28] V. Limongelli, L. Marinelli, S. Cosconati, H.A. Braun, B. Schmidt, E. Novellino, Chem. Med. Chem. 5 (2007) 667–678.
[29] E.F. Pettersen, T.D. Goddard, C.C. Huang, G.S. Couch, D.M. Greenblatt, E.C. Meng, T.E. Ferrin, J. Comput. Chem. 25 (2004) 1605–1612.